ACS Partner Journal

Journal of the American Society for Mass Spectrometry

pubs.acs.org/jasms

Article

Comparison of Partially Denatured Cytochrome *c* Structural Ensembles in Solution and Gas Phases Using Cross-Linking Mass Spectrometry

Rebecca L. Cain and Ian K. Webb*

Cite This: *J. Am. Soc. Mass Spectrom.* 2025, 36, 153−160

Read Online

ACCESS | Metrics & More | Article Recommendations | Supporting Information

ABSTRACT: Electrospray ionization mass spectrometry (ESI-MS) can retain intact protein structures, but details about partially folded and unfolded protein structures during and after introduction to the gas phase are elusive. Here we use ESI-MS with chemical cross-linkers to compare denatured cytochrome *c* structures in both solution and gas phases. Solution phase cross-linking prior to ESI captures solution phase structures, while gas phase cross-linking through ion/ion reactions in the trap cell captures gas phase structures. Comparing the ECD fragmentation of the cross-linked products under both conditions shows very similar cross-linker identifications, alluding to no major structural dissimilarities between solution and gas structures. Molecular modeling of the denatured protein using the identified cross-linked sites as distant restraints allows for visualization of the denatured structures to pinpoint where unfolding begins. Our data suggest that cytochrome *c* likely begins to unfold due to interior hydrophobic expansion, followed by α helical unfolding. This localization of structural changes is more specific than using CCS measurements alone.

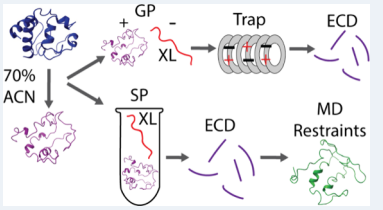

KEYWORDS: *ion mobility spectrometry, ion/ion reactions, native mass spectrometry, cross-linker, protein folding*

INTRODUCTION

Mass spectrometry is an informative tool for studying protein structure and folding/unfolding dynamics, especially for native proteins.[1] There is a wealth of information from native MS studies of proteins using electrospray ionization (ESI) since it can maintain intact protein structures as a soft ionization technique.[2] Bottom up approaches which combine methods such as chemical labeling, cross-linking, and hydrogen−deuterium exchange can be informative, but charge state related and intact structure information is lost.[3] Therefore, a top down approach is needed to provide the additional details from labeling and cross-linking experiments, while retaining the important information obtained from native mass spectrometry. Specifically, more insight is needed for denatured proteins as protein structure heavily influences protein function.[4] Protein stability depends on intramolecular interactions but also interactions with the solvent surrounding it, which also help to drive protein folding/unfolding.[5,6] During electrospray ionization (ESI), solvent evaporates as the ions enter the gas phase, leading to possible structural changes and multiple conformations.[5,7] Molecular dynamics studies have elucidated some of the details of how protein ions enter the gas phase. Two major models for protein ions are the charged residue model (CRM) in which nondenatured proteins are released into the gas phase after solvent evaporation and the chain ejection model (CEM) in which hydrophobic residues on denatured proteins migrate to the droplet surface and are ejected through electrostatic repulsion.[8] While denatured proteins are widely considered to enter the gas phase through CEM, more targeted work is needed on deciphering the changes denatured proteins undergo as they enter the gas phase.

There is also a strong correlation between the structural conformations of proteins and their charge states from electrospray measurements. Charge state distributions (CSDs) can be used to investigate solution phase conformational changes since number of charges on a protein can reflect the overall compactness.[9] Narrow CSDs centered around lower charge states are characteristic of folded proteins, while broader CSDs with higher charge states are characteristic of more unfolded proteins. Denatured protein studies to date have focused on the extent of unfolding rather than what specific conformational changes are occurring. For example, time-resolved studies by Konermann et al. (2006) used rapid mixing devices coupled with mass spectrometry, allowing for protein folding kinetic studies.[9]

Solution and gas phase chemical cross-linking, when coupled with top down mass spectrometry, can determine where and when structural changes may happen during the unfolding process and help to confirm protein structures.[10] Cross-linking

Received: September 19, 2024
Revised: November 20, 2024
Accepted: November 25, 2024
Published: December 12, 2024

involves covalently binding cross-linkers, most commonly involving commercially available lysine reactive reagents, with nearby residues to measure the distance between the residues in different conformations.[10] Cross-linking performed in solution occurs when cross-linkers are mixed prior to ionization. Cross-linking in the gas phase via ion/ion chemistry is performed when cross-linkers and molecules of interest are ionized separately and react in the gas phase. Previous work has optimized ion/ion reactions in the gas phase to cross-link after proteins are ionized.[11] These types of reactions allow for the "capture" of gas phase structures to help characterize conformations after ions are transferred in the gas phase, while solution cross-linking helps to "capture" solution phase conformations. Utilizing different length cross-linkers is also beneficial for identifying a range of different structures during the unfolding/refolding process.[12] Previous work done by Cheung See Kit et al. used different length cross-linkers for gas phase ion/ion reactions and found that cross-linking identification for native cytochrome *c* shows multiple, closely related conformational states.[11] Denatured proteins likely also present a mixture of conformational states, but the specific conformational differences between solution and gas phase structures need to be examined in greater detail. Distinguishing between solution and gas phase structures helps us to develop and evaluate structural mass spectrometry tools and measurements and allows us to learn more about the structural fates of ions in the gas phase. If structures are similar in both phases, the mass spectrometry measurements can be directly used in characterizing the protein structure. If not, then any major distinguishing features in protein structure between either phase need to be considered during structural interpretation.

This work used two different length cross-linkers for both solution and gas phase reactions with denatured cytochrome *c*. The cross-linked protein was then fragmented to locate where the cross-linkers bind for understanding which specific regions of the protein begin to unfold during denaturation. Solution phase cross-linking captured solution phase structures prior to ESI, while gas phase cross-linking occured after the protein ions entered the gas phase, capturing gas phase structures. By comparing the gas and solution phase cross-linking sites, we can then determine any structural changes that occur as proteins enter the gas phase.

METHODS

Reagents. Cytochrome *c* from bovine heart (Sigma-Aldrich; St. Louis, MO) solutions were prepared at 80 μM in water (pH 7) and diluted to 25 μM in 70:30 (vol:vol) acetonitrile (ACN, Fisher Scientific; Fairmont, NJ) and water. Lysine reactive cross-linkers bis(sulfosuccinimidyl)suberate (BS3, 11.4 Å) and bis(sulfosuccinimidyl) glutarate-d0 (BS2G, 7.7 Å) (Thermo Fisher Scientific. Fairmont, NJ) were made in stock solutions of 3 mM in water and stored in aliquots at −80 °C.

Solution and Gas Phase Reactions. For solution phase reactions, cross-linking (XL) solutions were diluted to 1 mM with 70:30 (vol:vol) acetonitrile and water and mixed with the protein solution in a 10:1 (XL:protein) ratio for approximately 10 min prior to electrospray ionization. The reaction mixture was quenched with acetic acid and then loaded into a pulled borosilicate tip for static nanoESI directly into a Waters Synapt G2-Si IM-MS (Wilmslow, U.K.) at 0.9−1.5 kV. The cross-linked charge states (modified protein) were isolated and subjected to electron capture dissociation (ECD) using an ExD cell (Agilent, Santa Clara, CA) with a filament current of 2.4 A for fragmentation.[13,14] As a control, denatured cytochrome *c*, prior to cross-linking, was ionized from borosilicate tips at 1.0 kV, where each charge state was isolated and subjected to ECD, to look at unreacted fragmentation patterns. Since solution phase cross-linking under the above conditions can produce products with zero, one, two, or more cross-link attachments, we isolated only the charge state corresponding to one cross-linker addition. Additional control experiments with native cytochrome *c* were performed to compare folded protein fragmentation patterns with partially unfolded fragmentation. Finally, solution cross-linking was also performed under native-like conditions in pure water.

For gas phase reactions, the denatured protein solution was sprayed in positive mode from an infusion line with 2.0 μL/min flow and sprayed from pulled fused silica tips at 2.0−2.5 kV. The diluted cross-linkers were sprayed in negative mode from pulled borosilicate tips at 0.9 kV. The procedure for gas-phase cross-linking via ion/ion chemistry has been described in detail.[14] Briefly, protein ions and anions were isolated in the quadrupole and stored in the trap cell to react in the gas phase. The product ions were also subjected to ECD for fragmentation. After gas phase cross-linking, the product ions are reduced by two charges.[14] To compare fragmentation patterns of the cross-linked ions, denatured cytochrome *c* was reacted with 1*H*,1*H*,2*H*,2*H*-perfluoro-1-octanol (PFO, Sigma-Aldrich, St. Louis, MO), as described in the gas phase reactions above, to charge reduce the ions without modification.[11] Gas phase cross-linking was also performed on cytochrome *c* ions electrosprayed from pure water solutions.

Data Analysis. ECD data for the unmodified and cross-linked ions were collected in triplicate. The fragmentation patterns for each set of data were annotated using Viewer (Agilent, Santa Clara, CA) and then manually verified. Fragments identified in two or more replicates were counted in the final fragmentation pattern. Final sequence fragmentation for both unmodified and cross-linked charge states was visualized using Prosight Lite.[15] To locate the most likely cross-linked sites, fragment intensities for unmodified and cross-linked protein precursor ions were compared (Supporting Table 1). Significant discontinuity in fragment ion intensities (reduction by a factor of 2 or above) and silencing of fragments for cross-linked data in two or more replicates indicated a likely cross-link. CCS distributions were calibrated as previously described.[16] CCS calculations were performed using a Collidoscope[17] with N_2 buffer gas on the Big Red 200 supercomputer at Indiana University.

Molecular Dynamic Simulations. The molecular dynamic simulations were run with Gromacs 2021[18] with the OPLS-AA[19] force field for a 673 ns run on Big Red 200 to simulate the cytochrome *c* (starting structure from PDB code 1HRC[20]) unfolding process in 70:30 (vol:vol) ACN:water. The heme was removed from the starting structure for the MD simulations. The identified cross-linked sites from the solution phase cross-linking were used as distance restraints between the Cα's of the cross-linked lysines, using 30.5 and 34.2 Å solution phase distances for BS2G and BS3, respectively. The frames from the simulation fitting the distance restraints were clustered based on RMSD and then used to visualize the structural ensemble of the partially unfolded protein in solution. The starting structure was the crystal structure of cytochrome *c* from equine heart with the heme removed.[21]

https://doi.org/10.1021/jasms.4c00388
J. Am. Soc. Mass Spectrom. 2025, 36, 153−160

Structures were visualized and analyzed in the open source build of PyMOL.

RESULTS AND DISCUSSION

Identifying Shifts in Electrospray Charge State and Collision Cross Section Distributions from Unfolding. Acidic conditions greatly reduce the reaction kinetics of NHS cross-linking; therefore, we used solutions of 70% acetonitrile at pH 7 to denature the protein as well as allow for cross-linking experiments to be conducted. Under organic denaturing conditions, cytochrome *c* shows a charge state distribution centered around the 9^+ charge state as compared to 7^+ charge state under native conditions (Figure 1),

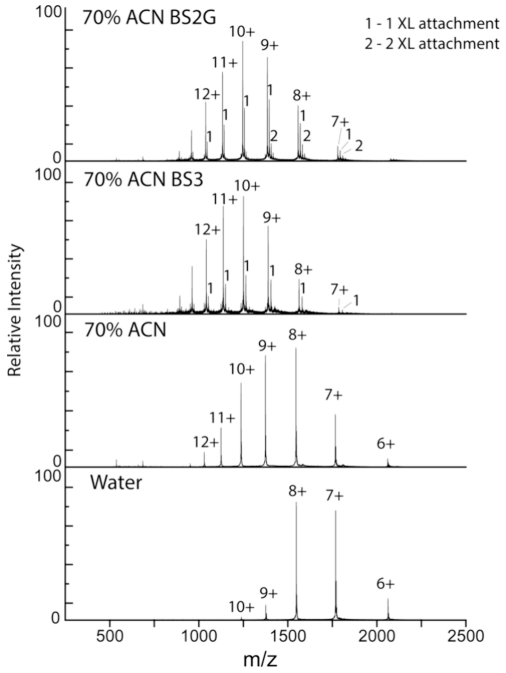

Figure 1. Charge state distribution of cytochrome *c* under denaturing (70% ACN) and native (water) conditions with no cross-linkers, with cross-linker BS3, and cross-linker BS2G. After denaturation, the charge state distribution shifts toward higher charge states. After cross-linking there is a mass shift according to the mass addition of the corresponding cross-linkers.

indicating partial denaturation, while still permitting cross-linking reactions. Along with the shift in charge states, the CSD also broadens to include higher charge states of 10^+ and 11^+. Denaturation of cytochrome *c* is known to disrupt intramolecular bonds, specifically through disruption of the iron to methionine 80 bond, thus shifting the charge state distribution toward higher charge states.[22] There is also a very slight shift in the CSD of the cross-linked protein due to the acid quenching step after cross-linking.

The nitrogen collision cross section (CCS) data for acetonitrile-denatured cytochrome *c* from calibrated traveling wave measurements show evidence for two major conformational families in charge states 7^+ through 11^+. The denatured 7^+ (1992 Å^2 and 2234 Å^2) and 8^+ (2136 Å^2 and 2547 Å^2) CCS values are larger than the native 7^+ (around 1400 Å^2) and 8^+ (around 1700 Å^2) CCS values from literature.[23,24] Larger CCS measurements correspond to more linear, unfolded charge states, so the larger CCS values shown for cytochrome *c* in ACN are an indication of partial unfolding. The 8^+ charge state represents a transition, with the inclusion of the higher feature at 2547 Å^2, and loss of the most compact feature present for the 7^+ charge state. The 9^+ charge state shows primarily the most extended state, maintained for 10^+ and 11^+ with CCS values of 2536 Å^2 and 2719 Å^2, respectively. As the charge increases in the denatured measurements, the conformational states expand, pointing to the most extended state in Figure 2 being generated in the gas phase via Coulombic repulsion, making it difficult to apply these CCS values directly to solution-like structures.[25]

Charge State	Mean CCS (Å^2)	CV (%)
11^+	2719	7
10^+	2536	5
9^+	A: 2443 B: 2574	1: 2 2: 9
8^+	A: 2136 B: 2547	A:9 B: 14
7^+	A: 1992 B: 2234	A:4 B:7

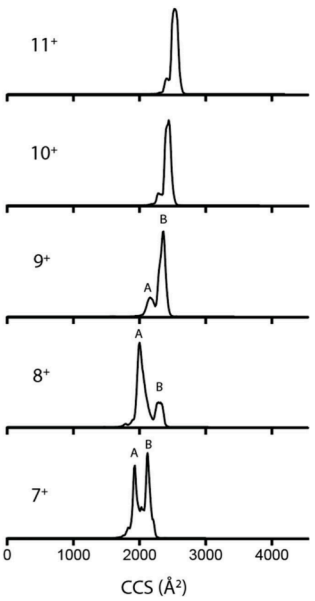

Figure 2. Calibrated CCS distributions for non-cross-linked charge states observed under partially denaturing conditions and tabulation of their mean values and coefficient of variance (CV (%)).

Solution and Gas Phase Cross-Linking Shifts Mass-to-Charge and Arrival Time Distributions. The extent of solution cross-linking was evaluated by examining the resulting cross-linking mass spectra. After solution cross-linking, cytochrome *c* shows mass shifts corresponding to the attached cross-linker (BS3 mass shifts of 138 *m*/*z* and BS2G mass shifts of 96 *m*/*z*) in addition to the remaining unmodified protein peaks. Each charge state had peaks for no cross-linker attached, one cross-linker, and two cross-linker attachments. The precursor peaks for attachment of a single cross-link were *m*/*z* isolated. ECD fragmentation was used to identify cross-linking sites. Solution phase cross-linking, at least for only one cross-link, does not change the arrival time distribution (ATD) for the cross-linked charge state versus the unmodified ion at the same charge. During gas phase cross-linking, charge states are isolated and then react with the isolated cross-linker dianions in the trap cell. The ion/ion product is an electrostatically, intramolecularly linked protein, with the sulfonates forming electrostatic bonds with protonated residues. Ion mobility separation after the reaction results in separate peaks for the non-cross-linked protein and cross-linked protein, since the reaction reduces charge by two (Supporting Figure 1). Cross-link attachment in the gas phase is confirmed through the multiple IM peaks and *m*/*z* shifts. For the gas phase reactions, the cross-linked and unmodified data are extracted from the mobility peak corresponding to one

https://doi.org/10.1021/jasms.4c00388
J. Am. Soc. Mass Spectrom. 2025, 36, 153−160

cross-linked attachment (Figure S2) to identify cross-linked and unmodified fragments.

Solution and Gas Phase Cross-Link Identification. The rest of this work focuses on comparison between lower charge states 7^+ and 8^+ and higher charge states 10^+ and 11^+ of acetonitrile denatured cytochrome *c* for better insight into the effects of charge and solvation as the ions enter the gas phase. Again, protein charge relates to protein conformation and higher charge states yield extended conformational states.[26] By comparing the higher and lower charge states, we can observe whether denatured conformational states follow this trend as well as see how different conformational states change after denaturation.

Each charge state of the unreacted protein showed fragmentation throughout (Figure 3, Supporting Figure 2).

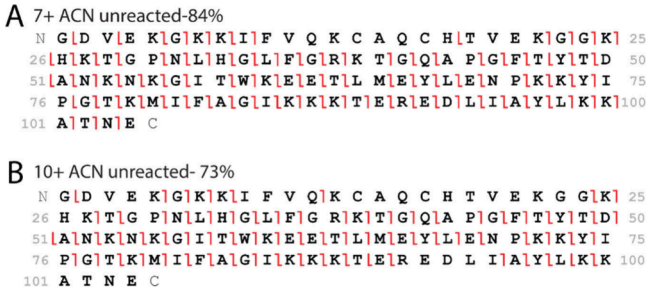

Figure 3. Sequence fragments for non-cross-linked 7^+ (A) and 10^+ (B) charge states of denatured cytochrome *c*.

Lack of fragmentation near C14 and C17 is likely due to the heme covalently bound to those cysteines.[24] This gap in fragmentation is seen in native, unreacted, and cross-linked data. Cross-linked data were compared with unreacted fragmentation and unmodified fragmentation. Comparisons within the same data set, referred to as unmodified data, differentiated fragments from cross-linked protein and from non-cross-linked protein in the same mixture.

We identified modified fragments that contained the cross-link attachment. Comparing modified and unmodified ECD fragmentation patterns and fragmentation intensities revealed the most likely cross-linked sites. As seen in Supplemental Table 1, fragmentation produced from unmodified protein produces high intensity fragments. Once a cross-link is attached, that region of the protein is "protected" from fragmentation as the cross-link secures that region of the protein. These protected regions are depicted in the gray boxes on the sequence coverage maps for Figures 4 and 5, showing the two cross-linked lysines with the protected region in between. Even though fragmentation still may be occurring, the cross-linker is bound to the two fragments, resulting in no change in *m*/*z*. This has a silencing effect, with modified fragmentation patterns producing significantly lower intensity fragments and/or no cross-linked fragments within that protected region. Combining the observation of where modified fragments began to appear as well as significant fragment silencing provided evidence for cross-linking sites.[11,14]

There is a potential to have a mixture of different cross-linked sites even with only a *m*/*z* shift for a single cross-link observed. To determine the most likely of these newly formed isomers, experimental fragmentation patterns were compared with denatured, non-cross-linked (unreacted data) (Figure 3)

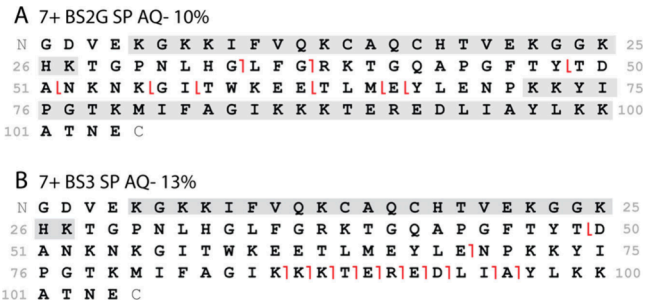

Figure 4. Sequence coverages for 7+ charge state of native cytochrome *c* cross-linked with BS2G (A) and BS3 (B) in solution. The gray boxes indicate the two cross-linked lysines, with the "protected" region in between.

and native, cross-linked protein (Figure 4) to ascertain the unique fragments and location of the cross-links. The overall charge state distribution reflects protein conformations after cross-linking, not necessarily the ensemble of structures prior to cross-linking. Looking at the cross-linking for each charge state gives information about where the cross-links attach for different conformations or whether various charge states in a unimodal distribution reflect different solution structures.

The most common regions of silencing between two lysine residues in two or more replicates of the same charge state were picked as the most common cross-link site (Table 1). For example, the 10^+ charge state when cross-linked with BS2G in solution had significant silencing between K7-39 and K72-86, K5-K27, and K7-27 for each replicate. Taken as a whole, these data suggest that the residues most commonly cross-linked under these conditions were K5-K27 (Figure 5). Cross-linking sites did not significantly change between native and denaturing conditions (Table 1), indicating a structurally dynamic N-terminus even for the native state. Cross-linked regions identified for each charge state were in the region of K5-K27 for both cross-linkers (Figure 5 and 7 and Supporting Figure 3). There appeared to be no correlation between charge state and solution phase structure, also in support of the hypothesis that changes in the average charge state of each component in the overall distribution,[26] not the individual charge states themselves, report on differences in solution structure. For gas phase cross-linking, the higher charge states (10+ and 11+) had cross-link identifications closer to the N-terminus, indicating similar cross-linking between the solution and the gas phase. The lower charge states (7+ and 8+) show cross-linking into the interior region in the sequence for the gas phase, indicating different cross-linking than what was observed in solution. Cross-linking in the interior of the protein for the lower charge states can be attributed to multiple mechanisms. The first possibility is structural collapse after ionization.[25,27,28] Cross-linking after this collapse would indicate the 7^+ and 8^+ charge states do not fully retain solution structural features. The 7^+ had identified cross-linked sites around K5-K73 for BS2G and K25-K73 for BS3 and the 8^+ had similar sites (Figure 5, Figure 6, and Supporting Figure 3). The fragment ion data from the gas phase cross-linking of the higher charge states suggested cross-linking in the N-terminal region. The 10+ charge state had cross-linked sites of K5-K39 for both cross-linkers (Figure 6), and the 11+ had sites of K5-K27 for both cross-linkers. In the gas phase, the higher charge states may avoid collapse due to charge repulsion, in contrast to the hypothesized compaction the 7^+ and 8^+ charge states

https://doi.org/10.1021/jasms.4c00388
J. Am. Soc. Mass Spectrom. 2025, 36, 153−160

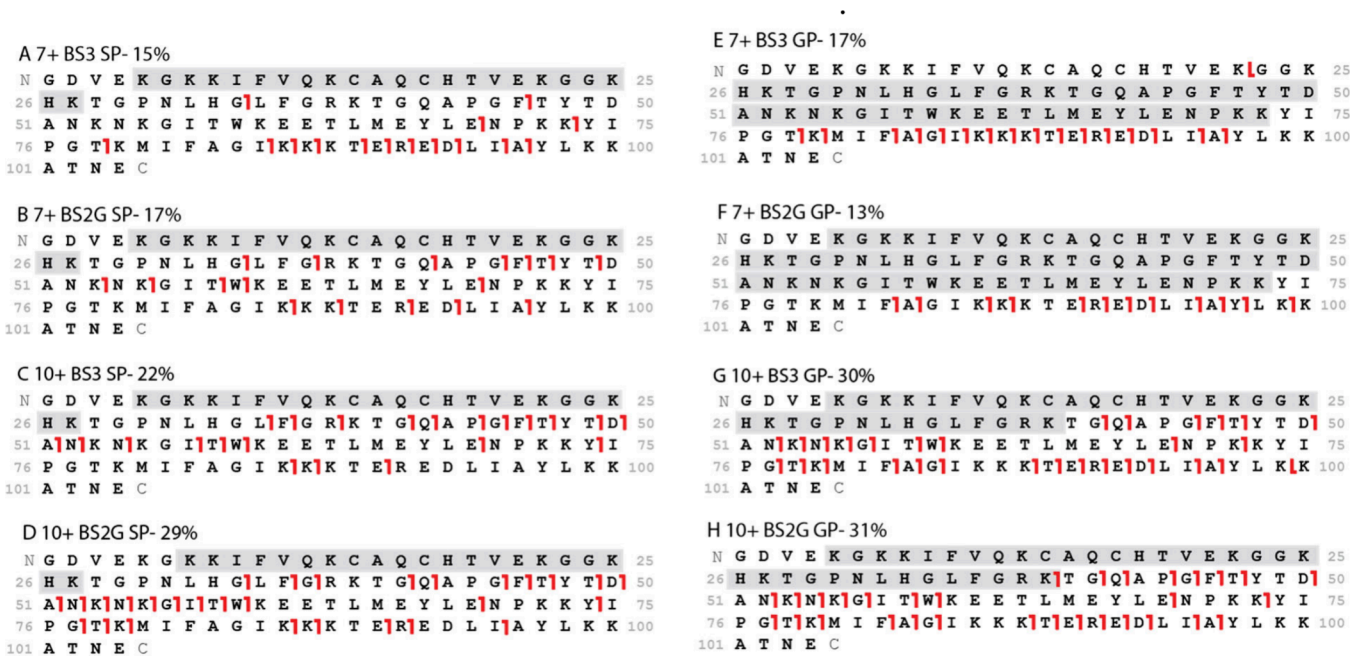

Figure 5. Denatured cytochrome *c* 7^+ and 10^+ sequence coverages for solution phase (A, B, C, D) and gas phase (E, F, G, H) cross-linking reactions with BS3 and BS2G. The two cross-linked lysines are depicted in the gray boxes, with the "protected" protein region in between.

Table 1. Summary of Identified Cross-Linked Sites from Solution and Gas Phase Cross-Linking Reactions[11]

	Under Denaturing Conditions	
charge state	solutuion phase XLs	gas phase XLs
7+	BS2G:K5-K27	BS2G:K5-K72
	BS3:K5-K27	BS3:K25-K72
8+	BS2G:K5-K27, K72-K100	BS2G:K5-K55
	BS3:K5-K27	BS3:K5-K39
10+	BS2G:K5-K27	BS2G:K5-K39
	BS3:K5-K27	BS3:K5-K39
11+	BS2G:K5-K27	BS2G:K5-K27
	BS3:K5-K25	BS3:K5-K27
	Under Native Conditions	
charge state	solutuion phase XLs	gas phase XLs
7+	BS2G:K5-K27, K72-K100	BS2G:K5-K27
	BS3:K5-K27	BS3:K25-K72
8+	BS3:K5-K27	

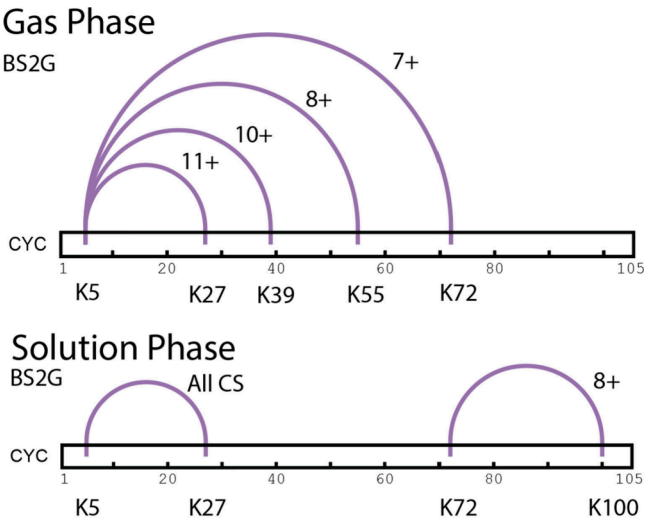

Figure 6. Cross-link visualization for BS2G for each cross-link identified for each charge state for solution phase (bottom) and gas phase (top) cross-linking under denaturing conditions.

experience. Our data could suggest that for partially unfolded proteins, the lowest charge states might not represent solution-like states and are overly compact compared to the actual solution states.

An alternative explanation is the cross-linkers span more distance in the gas phase than solution. The sulfo-NHS groups do not leave the cross-linkers during gas phase electrostatic cross-linking like they do in solution covalent cross-linking. Also, Coulombic interactions take place over very long ranges in the gas phase as they are not screened by ions and solvent like in solution. This results in the gas phase linkable Cα to Cα distance being 49.8 and 54.0 Å for BS2G and BS3, respectively, while solution phase linkable distances are 30.5 and 34.2 Å, respectively.[28] Therefore, our data may support partially unfolded structures for the low charge states of denatured cytochrome *c* and not support gas phase collapse. Cross-linking data from higher charge would then be evidence of more extended structures.

Discussion of Structural Changes for Denatured Cytochrome *c*. Similar cross-linked sites in two or more charge states for each cross-linker were used as the final distance restraints for the molecular dynamics-generated denatured structures. Cross-linked sites K5-27 and K5-39 were used to apply the distance restraints associated with the cross-linkers, BS3, 19.8 Å and BS2G, 15.6 Å. Structures (Figure 7) show partial denaturation compared to the native cytochrome *c* crystal structure. Native cytochrome *c* has five distinct α helices between residues D2-C14, T49-K55, K60-L68, N70–I75, and K87-E104, containing both the N- and C-termini. The modeled denatured structures show expansion in the protein interior as well as the unfolding of the main helical features. In addition to characterizing the starting structures of protein ions that enter the gas phase through ESI, the

https://doi.org/10.1021/jasms.4c00388
J. Am. Soc. Mass Spectrom. 2025, 36, 153−160

denatured cross-linking acts as a probe to determine what specific regions change during the unfolding process, as compared to only the overall structure/shape implied from CCS measurements (depending on whether aspects of the solution structure are retained). Under both native and denaturing conditions, the cross-linking sites are along the N-terminus. The similar cross-linking between native and denaturing conditions is likely due to the helical structures of cytochrome *c*'s termini already being slightly extended and the relative dynamicity of the termini (*vide supra*).[29] This can mean the unfolding process is driven by the expansion of the hydrophobic core, Since the cross-linking does not indicate major structural changes in the termini themselves during partial denaturation, our data agrees with previous literature for cytochrome *c* that indicates unfolding begins by expansion of the hydrophobic core.[30]

To provide evidence suggesting either gas phase collapse for the lower charge states or gas phase expansion for the higher charge states, we calculated CCS values directly from the modeled partially unfolded solution structures (Supporting Table 2). Although this treatment does not consider the structural transitions that occur while the protein ions are transferred from droplets to the gas phase, it can provide an estimation of the amount of gas phase compaction or extension.[25,27,28] The calculations show that the representative structures include a range of CCS values from roughly 1900 to 2200 Å^2 for charge states 7^+ and 8^+ and from 2000 to 2300 Å^2 for charge states 10^+ and 11^+. Higher charge results in stronger ion−dipole interactions with nitrogen which increases the CCS for higher charge states even if there are no changes in the overall size/shape of the ion.[31] These CCS values are in close agreement with the measured CCS of the more compact of the conformer families for 7^+ and 8^+ from Figure 2. However, the measured CCS values of the higher charge states were significantly higher than the calculated values, suggesting that the 10^+ and 11^+ charge states undergo significant gas phase expansion. Finally, the representative structures from Figure 7

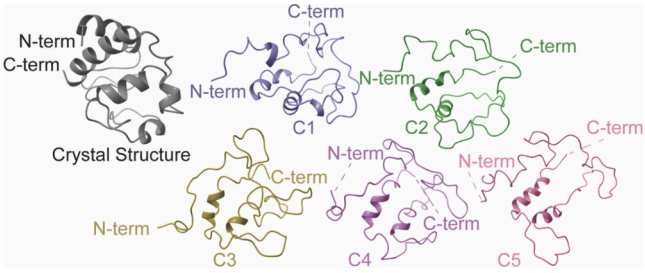

Figure 7. Crystal structure of cytochrome *c* and representative structures from clustered molecular dynamics simulation representing partially unfolded cytochrome *c* in agreement with solution phase cross-linking assignments. Protein N- and C-termini are labeled in the figure for clarity.

were analyzed in PyMOL to determine whether the gas phase cross-linking for the lower charge states was in support of maintaining solution-like partially unfolded structures in the gas phase (Supporting Table 3). All of the lysine to lysine Cα to Cα distances bridged by the gas phase cross-links for the 7^+ and 8^+ charge states were found to be within the maximum lengths of the gas phase cross-linkers. Thus, our data suggest that cytochrome *c*, a cationic protein in solution, maintains solution-like structures in the gas phase under both native and partially unfolded conditions at the lowest charge states, while the structures with higher charge undergo significant expansion in the gas phase.

CONCLUSION

Denaturing cytochrome *c* with organic cosolvents while avoiding changes in pH partially unfolds the protein while still allowing cross-linking reactions. Under these denaturing conditions, cross-linking in both solution and gas phases produces similar cross-linked sites for higher charge states but linking into the interior of the protein with the lower charge states. This was most likely due to the electrostatic reagents being significantly larger in the gas phase, due to both the retention of the sulfo-NHS groups as well as the long lengths of electrostatic interactions in the gas phase between sulfo-NHS and positively-charged residues. Thus, future work will include the development of covalent gas-phase ion/ion cross-linking strategies suitable for the reaction timescales on our IM-MS instrument. Comparing the denatured conditions to native conditions also reveals similar cross-linking patterns, meaning the unfolding process is driven by internal expansion rather than unfolding at either terminus, since the termini are mainly helical in the crystal structure, indicating that they are "extended" even in native-like forms.

The transfer of compact, native-like proteins to the gas phase does not significantly alter or disrupt intermolecular bonds. Additionally, our cross-linking and CCS data presented here with the help of molecular dynamics and CCS calculations suggest that partially unfolded gas phase protein ions also can maintain many aspects of their solution structure at low charge. Based on ours and previous studies, it seems like whether this is true is protein dependent and is best ascertained by a combination of multiple solution and gas phase experimental techniques. The continued development of gas phase molecular modeling, CCS calculators, and complementary gas phase tools will continue to be needed to characterize structurally dynamic systems.

ASSOCIATED CONTENT

Data Availability Statement

The raw mass spectra will be made available in a public repository before publication.

Supporting Information

The Supporting Information is available free of charge at https://pubs.acs.org/doi/10.1021/jasms.4c00388.

ATDs of cross-linked products, ECD sequence coverages for cross-linked and unmodified cytochrome *c*, and CCS and distances of the representative structures from MD (PDF)

AUTHOR INFORMATION

Corresponding Author

Ian K. Webb − *Department of Chemistry and Chemical Biology, Indiana University—Indianapolis, Indianapolis, Indiana 46202, United States; Center for Computational Biology and Bioinformatics, Indiana University School of Medicine, Indianapolis, Indiana 46202, United States;* orcid.org/0000-0001-7223-8729; Email: ikwebb@iu.edu

https://doi.org/10.1021/jasms.4c00388
J. Am. Soc. Mass Spectrom. 2025, 36, 153−160

Author

Rebecca L. Cain − *Department of Chemistry and Chemical Biology, Indiana University—Indianapolis, Indianapolis, Indiana 46202, United States*

Complete contact information is available at: https://pubs.acs.org/10.1021/jasms.4c00388

Notes

The authors declare no competing financial interest.

■ ACKNOWLEDGMENTS

This work was supported by the National Science Foundation under Grant CHE 2143755. This research was supported in part by Lilly Endowment, Inc., through its support for the Indiana University Pervasive Technology Institute.

■ REFERENCES

(1) Bakhtiari, M.; Konermann, L. Protein Ions Generated by Native Electrospray Ionization: Comparison of Gas Phase, Solution, and Crystal Structures. *J. Phys. Chem. B* **2019**, *123* (8), 1784−1796.

(2) Loo, J. A.; Edmonds, C. G.; Smith, R. D. Primary sequence information from intact proteins by electrospray ionization tandem mass spectrometry. *Science* **1990**, *248* (4952), 201−204. Heck, A. J.; Van Den Heuvel, R. H. Investigation of intact protein complexes by mass spectrometry. *Mass Spectrom. Rev.* **2004**, *23* (5), 368−389.

(3) Kelleher, N. L.; Lin, H. Y.; Valaskovic, G. A.; Aaserud, D. J.; Fridriksson, E. K.; McLafferty, F. W. Top down versus bottom up protein characterization by tandem high-resolution mass spectrometry. *J. Am. Chem. Soc.* **1999**, *121* (4), 806−812.

(4) Farmer, T. B.; Caprioli, R. M. Determination of protein−protein interactions by matrix-assisted laser desorption/ionization mass spectrometry. *Journal of mass spectrometry* **1998**, *33* (8), 697−704. Bellissent-Funel, M.-C.; Hassanali, A.; Havenith, M.; Henchman, R.; Pohl, P.; Sterpone, F.; Van Der Spoel, D.; Xu, Y.; Garcia, A. E. Water determines the structure and dynamics of proteins. *Chem. Rev.* **2016**, *116* (13), 7673−7697. Xiao, Y.; Konermann, L. Protein structural dynamics at the gas/water interface examined by hydrogen exchange mass spectrometry. *Protein Sci.* **2015**, *24* (8), 1247−1256.

(5) Makhatadze, G. I.; Privalov, P. L. Contribution of hydration to protein folding thermodynamics. I. The enthalpy of hydration. *J. Mol. Biol.* **1993**, *232*, 639. Levy, Y.; Onuchic, J. N. Water mediation in protein folding and molecular recognition. *Annu. Rev. Biophys.* **2006**, *35*, 389.

(6) Kauzmann, W. Some factors in the interpretation of protein denaturation. *Adv. Protein Chem.* **1959**, *14*, 1.

(7) Grandori, R. Origin of the conformation dependence of protein charge-state distributions in electrospray ionization mass spectrometry. *J. Mass Spectrom.* **2003**, *38*, 11. Wyttenbach, T.; Bowers, M. T. Structural stability from solution to the gas phase: native solution structure of ubiquitin survives analysis in a solvent-free ion mobility-mass spectrometry environment. *J. Phys. Chem. B* **2011**, *115* (42), 12266−12275. Suckau, D.; Shi, Y.; Beu, S. C.; Senko, M. W.; Quinn, J. P.; Wampler, F. M.; McLafferty, F. W. Coexisting stable conformations of gaseous protein ions. *Proc. Natl. Acad. Sci. U. S. A.* **1993**, *90* (3), 790.

(8) Konermann, L.; Metwally, H.; Duez, Q.; Peters, I. Charging and supercharging of proteins for mass spectrometry: recent insights into the mechanisms of electrospray ionization. *Analyst* **2019**, *144* (21), 6157−6171. Peschke, M.; Verkerk, U. H.; Kebarle, P. Features of the ESI mechanism that affect the observation of multiply charged noncovalent protein complexes and the determination of the association constant by the titration method. *J. Am. Soc. Mass Spectrom.* **2004**, *15* (10), 1424−1434. From NLM.

(9) Konermann, L.; Pan, J.; Wilson, D. J. Protein Folding Mechanisms Studied by Time-Resolved Electrospray Mass Spectrometry. *BioTechniques* **2006**, *40* (2), 135−141.

(10) Leavell, M. D.; Novak, P.; Behrens, C. R.; Schoeniger, J. S.; Kruppa, G. H. Strategy for selective chemical cross-linking of tyrosine and lysine residues. *J. Am. Soc. Mass Spectrom.* **2004**, *15* (11), 1604−1611.

(11) Cheung See Kit, M.; Webb, I. K. Application of Multiple Length Cross-linkers to the Characterization of Gaseous Protein Structure. *Anal. Chem.* **2022**, *94* (39), 13301−13310.

(12) Politis, A.; Stengel, F.; Hall, Z.; Hernandez, H.; Leitner, A.; Walzthoeni, T.; Robinson, C. V.; Aebersold, R. A mass spectrometry-based hybrid method for structural modeling of protein complexes. *Nat. Methods* **2014**, *11* (4), 403−406. Novak, P.; Young, M. M.; Schoeniger, J. S.; Kruppa, G. H. A Top-Down Approach to Protein Structure Studies Using Chemical Cross-Linking and Fourier Transform Mass Spectrometry. *Eur. J. Mass Spectrom.* **2003**, *9* (6), 623−631.

(13) Williams, J. P.; Morrison, L. J.; Brown, J. M.; Beckman, J. S.; Voinov, V. G.; Lermyte, F. Top-Down Characterization of Denatured Proteins and Native Protein Complexes Using Electron Capture Dissociation Implemented within a Modified Ion Mobility-Mass Spectrometer. *Anal. Chem.* **2020**, *92* (5), 3674−3681.

(14) Cheung See Kit, M.; Carvalho, V. V.; Vilseck, J. Z.; Webb, I. K. Gas-Phase Ion/Ion Chemistry for Structurally Sensitive Probes of Gaseous Protein Ion Structure: Electrostatic and Electrostatic to Covalent Cross-Linking. *Int. J. Mass Spectrom.* **2021**, *463*, 116549−116559.

(15) Fellers, R. T.; Greer, J. B.; Early, B. P.; Yu, X.; LeDuc, R. D.; Kelleher, N. L.; Thomas, P. M. ProSight Lite: graphical software to analyze top-down mass spectrometry data. *Proteomics* **2015**, *15* (7), 1235−1238.

(16) Carvalho, V. V.; See Kit, M. C.; Webb, I. K. Ion Mobility and Gas-Phase Covalent Labeling Study of the Structure and Reactivity of Gaseous Ubiquitin Ions Electrosprayed from Aqueous and Denaturing Solutions. *J. Am. Soc. Mass Spectrom.* **2020**, *31* (5), 1037−1046. Sun, Y.; Vahidi, S.; Sowole, M. A.; Konermann, L. Protein Structural Studies by Traveling Wave Ion Mobility Spectrometry: A Critical Look at Electrospray Sources and Calibration Issues. *J. Am. Soc. Mass Spectrom.* **2016**, *27* (1), 31−40.

(17) Ewing, S. A.; Donor, M. T.; Wilson, J. W.; Prell, J. S. Collidoscope: An Improved Tool for Computing Collisional Cross-Sections with the Trajectory Method. *J. Am. Soc. Mass Spectrom.* **2017**, *28* (4), 587−596.

(18) Abraham, M. J.; Murtola, T.; Schulz, R.; Páll, S.; Smith, J. C.; Hess, B.; Lindahl, E. GROMACS: High performance molecular simulations through multi-level parallelism from laptops to supercomputers. *SoftwareX* **2015**, *1−2*, 19−25.

(19) Jorgensen, W. L.; Maxwell, D. S.; Tirado-Rives, J. Development and Testing of the OPLS All-Atom Force Field on Conformational Energetics and Properties of Organic Liquids. *J. Am. Chem. Soc.* **1996**, *118* (45), 11225−11236.

(20) Bushnell, G. W.; Louie, G. V.; Brayer, G. D. High-resolution three-dimensional structure of horse heart cytochrome c. *J. Mol. Biol.* **1990**, *214* (2), 585−595.

(21) Rolland, A. D.; Prell, J. S. Computational Insights into Compaction of Gas-Phase Protein and Protein Complex Ions in Native Ion Mobility-Mass Spectrometry. *Trends Analyt Chem.* **2019**, *116*, 282−291. PubMed.

(22) Englander, S. W.; Sosnick, T. R.; Mayne, L. C.; Shtilerman, M.; Qi, P. X.; Bai, Y. Fast and Slow Folding in Cytochrome c. *Acc. Chem. Res.* **1998**, *31* (11), 737−744. Cain, R.; Webb, I. Online Protein Unfolding Characterized by Ion Mobility Electron Capture Dissociation Mass Spectrometry: Cytochrome C from Neutral and Acidic Solutions. *Anal. Bioanal. Chem.* **2023**, *415*, 749−758.

(23) May, J. C.; Jurneczko, E.; Stow, S. M.; Kratochvil, I.; Kalkhof, S.; McLean, J. A. Conformational Landscapes of Ubiquitin, Cytochrome c, and Myoglobin: Uniform Field Ion Mobility Measurements in Helium and Nitrogen Drift Gas. *Int. J. Mass Spectrom.* **2018**, *427*, 79−90.

(24) Zhuang, J.; Amoroso, J. H.; Kinloch, R.; Dawson, J. H.; Baldwin, M. J.; Gibney, B. R. Evaluation of Electron-Withdrawing

Group Effects on Heme Binding in Designed Proteins: Implications for Heme a in Cytochrome c Oxidase. *Inorganic* **2006**, *45*, 4685−4694.
(25) Vahidi, S.; Stocks, B. B.; Konermann, L. Partially Disordered Proteins Studied by Ion Mobility-Mass Spectrometry: Implications for the Preservation of Solution Phase Structure in the Gas Phase. *Anal. Chem.* **2013**, *85* (21), 10471−10478.
(26) Li, J.; Santambrogio, C.; Brocca, S.; Rossetti, G.; Carloni, P.; Grandori, R. Conformational effects in protein electrospray-ionization mass spectrometry. *Mass Spectrom. Rev.* **2016**, *35* (1), 111−122.
(27) Pagel, K.; Natan, E.; Hall, Z.; Fersht, A. R.; Robinson, C. V. Intrinsically disordered p53 and its complexes populate compact conformations in the gas phase. *Angew. Chem., Int. Ed. Engl.* **2013**, *52* (1), 361−365.
(28) Cheung See Kit, M.; Cropley, T. C.; Bleiholder, C.; Chouinard, C. D.; Sobott, F.; Webb, I. K. The role of solvation on the conformational landscape of α-synuclein. *Analyst* **2023**, *149* (1), 125−136.
(29) Colón, W.; Elöve, G. A.; Wakem, L. P.; Sherman, F.; Roder, H. Side chain packing of the N-and C-terminal helices plays a critical role in the kinetics of cytochrome c folding. *Biochemistry* **1996**, *35* (17), 5538−5549.
(30) Akiyama, S.; Takahashi, S.; Ishimori, K.; Morishima, I. Stepwise formation of alpha-helices during cytochrome c folding. *Nat. Struct. Biol.* **2000**, *7* (6), 514−520. From NLM.
(31) Canzani, D.; Laszlo, K. J.; Bush, M. F. Ion Mobility of Proteins in Nitrogen Gas: Effects of Charge State, Charge Distribution, and Structure. *J. Phys. Chem. A* **2018**, *122* (25), 5625−5634.

https://doi.org/10.1021/jasms.4c00388
J. Am. Soc. Mass Spectrom. 2025, 36, 153−160